Polymer Bulletin (2026) 83:251
https://doi.org/10.1007/s00289-025-06184-6

ORIGINAL PAPER

Crosslinked poly(vinyl alcohol) membranes containing imidazole/pyridine side chains for high temperature proton exchange membrane fuel cells

Peiru Lv[1] · Li Ning[1] · Danni Wu[2] · Qi Liao[1] · Jin Wang[2] · Jingshuai Yang[1]

Received: 12 December 2024 / Revised: 16 May 2025 / Accepted: 22 September 2025

Abstract

A series of poly(vinyl alcohol) (PVA) based membranes for high temperature proton exchange membrane fuel cells are synthesized via a simple aldol condensation reaction. Three aldehyde compounds with alkaline groups, including 4-(bromomethyl) benzaldehyde grafted with 1-methylimidazole (QBMB-MeIm), 4-pyridinecarboxaldehyde (4PCA), and 4-(1H-imidazol-1-yl)benzenecarbaldehyde (4IBA), are grafted onto the PVA main chain, while glutaraldehyde (GA) is used as a crosslinking agent to improve the mechanical properties of the membranes. A systematic investigation was conducted on these crosslinked membranes to evaluate the influence of different side-chain groups and crosslinking degrees on their properties. The imidazole and pyridine groups on the PVA side chains enhance phosphoric acid (PA) absorption, resulting in excellent proton conductivity and acid doping capability. Among the synthesized membranes, PVA-4IBA-20%GA exhibits the best performance, achieving 220% PA uptake when immersed in 85 wt% PA at 30 °C. It also demonstrates a tensile strength of 3.7 MPa and a conductivity of up to 0.158 S cm^{-1} at 150 °C. These findings highlight the significant potential of PVA-based membranes for HT-PEMFC applications, offering a promising avenue for future energy technologies.

Keywords High temperature proton exchange membranes · Poly(vinyl alcohol) · Side chain grafting · Aldol condensation reaction

✉ Jin Wang
wangjin@symc.edu.cn

✉ Jingshuai Yang
yjs@mail.neu.edu.cn

[1] Department of Chemistry, College of Sciences, Northeastern University, Shenyang 110819, China

[2] College of Pharmacy, Shenyang Medical College, Shenyang 110034, China

Published online: 09 February 2026

Introduction

With the worsening of environmental pollution and the depletion of traditional energy sources like fossil fuels, exploring green fuels and efficient energy conversion technologies has become a critical challenge of the twenty-first century. Hydrogen, which can be produced by water electrolysis using renewable electricity, stands out as a promising green fuel [1]. Fuel cells powered by hydrogen offer advantages such as high conversion efficiency, minimal harmful gas emissions, low environmental pollution, and long service life, making them promising energy devices [2, 3].

Proton exchange membrane fuel cells (PEMFCs) possess advantages like zero emissions, high power density, and superior climate adaptability, positioning them as a leading power sources option for electric vehicles [4, 5]. High-temperature PEMFCs (HT-PEMFCs), working at temperatures above 100 °C, offer several benefits over low-temperature PEMFCs. For example, HT-PEMFCs exhibit enhanced electrode reaction kinetics, higher electrode tolerance to CO, and a relatively simple hydrothermal management system [6, 7]. The high-temperature proton exchange membrane (HT-PEM) plays a pivotal role in HT-PEMFCs; it not only serves as a barrier but also facilitates proton conduction from the anode to the cathode while remaining chemically inert and managing water and heat distribution [8–10]. Therefore, the HT-PEM should have good proton conductivity, excellent electrochemical stability, and reasonable mechanical strength.

Currently, Nafion membranes are widely used because of their excellent conductivity and strong mechanical and electrochemical stability [9, 11, 12]. Nevertheless, issues like the high expense, fuel crossover problems due to membrane dehydration under high operating temperatures, and significant degradation have hindered the industrial application of Nafion membranes [9, 13]. Therefore, exploring alternative membrane materials that can replace Nafion is necessary to achieve practical applications and large-scale commercialization of fuel cells [14]. Up to now, fluorine-free polymers have also been widely investigated, such as sulfonated polyether ether ketone (SPEEK) and sulfonated polyaryl ether sulfone (SPES) [15]. For instance, Keshk et al. [16] utilized layered double hydroxide/sepiolite nanostructures to enhance the performance of SPEEK membranes at elevated temperatures. Among all potential candidate materials, poly(vinyl alcohol) (PVA) membranes, which exhibit low fuel permeability, excellent mechanical, chemical, and thermal stability, good film-forming ability, relatively low production cost, and hydroxyl groups that can act as proton transfer bridges, meet the requirements for alternative membrane materials and show great potential in fuel cell applications [17–19].

The presence of hydroxyl groups allows for the modification of PVA with aldehydes via acetal functionalization [20]. Multiple PVA derivatives have been successfully produced using acetalization reagents such as 4-formyl-1-methylpyridinium [21], 4-dimethylaminobenzaldehyde [20, 22], imidazole-4-carbaldehyde [23], 1-methyl-2-imidazolecarboxaldehyde [24], 4-(bromomethyl)benzaldehyde [25] and 4-imidazolyl benzaldehyde [26]. Recently, PVA has garnered significant attention and developed as a polymer electrolyte membrane for fuel cells [18]. For instance, Rao et al. [27] prepared a PVA-coated Nafion membrane used as an anion exchange membrane (AEM) in a fuel cell, significantly reducing methanol cross-

over. Keshk et al. [28] prepared optically tunable and proton-conductive multivalent metal chloride-loaded oxide PVA hybrid membranes, demonstrating enhanced proton conductivity through ionic radius modulation of doped cations. Pivovar et al. [29] showed that PVA membranes exhibit lower proton conductivity compared to Nafion™ membranes due to the absence of negatively charged ions in PVA. Therefore, it is necessary to modify PVA by adding proton sources to improve its proton conductivity and hydrophilicity. According to Ye et al. [30], the swelling, chemical, and mechanical characteristics of polymer membrane materials can be effectively controlled by adjusting the crosslinking degree of the PVA base membrane to modify the dense molecular network structure. These examples indicate the promising role of PVA-based polymer membranes as separation materials in energy conversion and storage applications. Nonetheless, to our knowledge, limited studies have been reported on the use of PVA-based membranes for PEMFCs.

In the present work, we used PVA as the backbone and linked different basic groups to its side chains through aldol condensation reactions. Glutaraldehyde (GA) solutions of different concentrations were used as crosslinking agents to prepare crosslinked membranes via chemical crosslinking, aiming to study the effects of different side-chain groups and varying degrees of crosslinking on the properties of the membrane materials. Crosslinking the modified membranes can produce more compact or denser structures, improving the structural strength of the membranes. The imidazole and pyridine groups on the side chains of the PVA-based membranes prepared in this study can effectively adsorb phosphoric acid, exhibiting good acid doping ability and good proton conducting properties.

Experimental

Materials

Poly(vinyl alcohol) (PVA), 4-(1H-imidazol-1-yl)benzenecarbaldehyde (4IBA), 1-methylimidazole (MeIm), and glutaraldehyde (GA) were purchased from J&K Scientific. 4-(Bromomethyl)benzaldehyde (QBMB) was obtained from Adamas Reagent Ltd., and 4-pyridinecarboxaldehyde (4PCA) was sourced from Energy Chemical. Phosphoric acid (PA, 85 wt%) were provided by Sinopharm Chemical Reagent Co. Ltd., and dimethyl sulfoxide (DMSO), methanol (MeOH), sodium hydroxide (NaOH), hydrochloric acid (HCl, 37 wt%). All chemicals were employed directly without additional purification.

Synthesis of grafted polymers

The PVA grafted with QBMB and MeIm was synthesized following the methods described in the literature [25]. The synthesis of PVA grafted with 4PCA and 4IBA polymers proceeded as follows: A total of 2.00 g PVA and 45.5 mL DMSO were added to a 100 mL three-neck flask. The mixture was stirred magnetically under reflux at 50 °C until the PVA was completely dissolved, forming a clear solution. Ten milliliters of this PVA solution were transferred to a reagent bottle, and a drop

of 37 wt% HCl was added to adjust the pH. After thorough mixing, an appropriate amount of 4PCA or 4IBA was added to the mixture. The mixture was then stirred and heated at 50 °C under constant reflux for 72 h, resulting in a clear yellow solution. Once the reaction was complete, the mixture was cooled and gradually added to an aqueous NaOH solution to precipitate yellow flocculent fibers. The precipitate was allowed to settle, then filtered and rinsed with deionized water 2–3 times to eliminate residual reagents. Resulting product was thoroughly dried for 12 h to obtain a yellowish solid.

Preparation and crosslinking of membranes

Membranes were prepared using a solution-casting technique. The grafted polymer was dissolved in DMSO to form a 2.0 wt% solution under magnetic stirring at 80 °C. Once a homogeneous solution was achieved, it was poured onto Teflon Petri dishes and the solvent was evaporated at 60 °C in an oven until fully removed. The membranes were then removed, thoroughly washed with deionized water, and then dried to obtain homogeneous and transparent membranes. For the PVA grafted with QBMB, the product exhibited poor solubility. Therefore, after grafting, the product was not precipitated but directly poured into Teflon Petri dishes to form membranes. The resulting membrane was then soaked in a methanol solution of MeIm for 12 h to complete further grafting. The corresponding membranes were designated as PVA-QBMB-MeIm, PVA-4PCA, and PVA-4IBA. The grafted membranes underwent crosslinking by being immersed in GA solutions of varying concentrations (10 wt%, 20 wt%, and 30 wt%) at 30 °C for 1 h. This process yielded crosslinked PVA membranes with different degrees of crosslinking, allowing the study of how crosslinking concentration affects membrane properties.

Acid and water doping and swelling

The completely dried membranes were soaked in an 85 wt% phosphoric acid (PA) solution within a vacuum oven at 30 °C until their masses remained constant. Excess PA on the surface was removed using filter paper. Measure the weight and dimensions of the membrane after thoroughly removing its moisture. The acid doping content (ADC%) was determined by calculating the ratio of the mass of doped acid to the dry mass of the membranes, according to Eq. (1) [31]. The area swelling degree (S) and volume swelling degree (V) in 85 wt% PA solution were calculated by assessing the dimensional changes of the membranes prior to and following PA swelling, determined by Eqs. (2) and (3), respectively, as in previous works [32, 33].

$$ADC/\% = \frac{m_{PA} - m_0}{m_0} \times 100\% \tag{1}$$

$$S/\% = \frac{S_{PA} - S_0}{S_0} \times 100\% \tag{2}$$

$$V/\% = \frac{V_{PA} - V_0}{V_0} \times 100\% \tag{3}$$

In Eq. (1), m_0 and m_{PA} represent the membrane mass prior to and following PA doping, respectively. S_0 and S_{PA} denote the membrane area before and after immersion in the PA solution, as per Eq. (2). Meanwhile, V_0 and V_{PA} represent the membrane volume prior to and following immersion in the PA solution, as per Eq. (3).

Similar to the measurements for ADC% and swelling in 85 wt% PA solution, water uptake (WU), water area swelling (WA), and water volume swelling (WV) were determined in deionized water as previously described [34, 35].

Characterizations

The ion exchange capacity (IEC) of the PVA-QBMB-MeIm-20%GA membrane was determined using a precipitation titration method [36]. Membrane samples were immersed in 0.5 mol L^{-1} $NaNO_3$ for 48 h at room temperature, followed by titration with 0.1 mol L^{-1} $AgNO_3$. The IEC was calculated using Eq. (4).

$$IEC = \frac{V \times c}{m} \tag{4}$$

where V is the volume of $AgNO_3$ solution used, c is its concentration, and m is the membrane mass.

The solubility of various membranes was tested by soaking the membrane samples in DMSO for 12 h at 60 °C. The mass retention rate (MR) of the membranes was calculated by Eq. (5).

$$MR = \frac{m_1}{m} \times 100\% \tag{5}$$

where m_1 represents the mass of the membrane sample after soaking in DMSO, and m represents the initial mass of the membrane sample.

To evaluate PA retention under high temperature and humidity, membranes were kept at 80 °C and 40% RH. The retention rate was calculated as.

$$\text{PA retention rate} = \frac{ADC_t}{ADC_0} \times 100\% \tag{6}$$

where ADC_0 is the initial acid content and ADC_t is the acid content after t hours.

The ^{1}H NMR spectra of the polymers were obtained on a Bruker AVANCE 600 MHz spectrometer, using tetramethylsilane (TMS) as the internal reference and deuterated dimethyl sulfoxide (DMSO-d_6) as the solvent. Fourier transform infrared (FT-IR) spectra were recorded using a Bruker VERTEX70 spectrometer, utilizing a DTGS detector and a ZnSe crystal as an attenuated total reflection (ATR) accessory. Surface and cross-sectional morphologies of the membranes were observed using scanning electron microscopy (SEM, SU-8010). Prior to SEM examination, the sam-

ples were sputter-coated with platinum in a vacuum environment. The chemical stability of the membrane was evaluated by the mass retention rate after immersing it in Fenton reagent containing 3.0% H_2O_2 and 4.0 ppm Fe^{2+} at 80 °C. Thermogravimetric analysis (TGA) was conducted using a METTLER-TOLEDO (HT/808) instrument from 30 to 800 °C at a heating rate of 10 °C min^{-1} under a nitrogen atmosphere.

Stress–strain curves were obtained using a tensile testing device (CMT2000, SHIJIN Company, China) with a constant speed of 5 mm min^{-1} under ambient conditions. All membrane samples were shaped into dumbbells, with the middle section measuring 2.5 cm long and 0.4 cm wide.

The proton conductivities of the PA-doped membranes were measured using a four-electrode technique at a frequency of 4 kHz and a voltage of 2 V [37, 38]. Before measuring conductivity, all membranes were dried at 100 °C for 2 h to remove any influence of water. The measurements were conducted in an oven with ambient air and no humidification, with the temperature controlled from 100 to 150 °C. The resistances were recorded at every 10 °C increment. The proton conductivity (σ) was calculated according to Eq. (7):

$$\sigma = \frac{L}{RS} \tag{7}$$

In Eq. (7), R represents the resistance of the membrane, L represents the distance between electrodes, while S is the cross-sectional area of the membrane.

Results and discussion

Micromorphology of membranes

In this paper, PVA was grafted with aldehydes containing different basic groups and crosslinked with GA solutions of varying concentrations to prepare a series of membranes with basic groups, as shown in Fig. 1. The obtained polymers exhibited excellent solubility in DMSO, which is conducive to membrane preparation via the solution-casting method, resulting in membranes of uniform thickness. It should be noted that PVA is practically insoluble in water at room temperature, washing at this temperature does not result in significant loss. However, PVA is partially soluble in hot water (~80 °C) as demonstrated by the solubility experiments as shown in Fig. S1 in the Supporting Information.

Figure 2 presents digital photographs alongside SEM images of all membranes. The figure illustrates that, all the membranes have a pale yellow, uniform, and diaphanous appearance. Additionally, SEM images of the surfaces of all the membranes reveal a dense and non-porous microstructure, which facilitates the separation of feed gas in fuel cells [8]. Figure S2 displays cross-sectional SEM and elemental distribution images of the PVA-4IBA-20%GA, PVA-QBMB-MeIm-20%GA, and PVA-4PCA-20%GA membranes. All membranes exhibited smooth cross-sections with uniform elemental distribution, indicating good homogeneity.

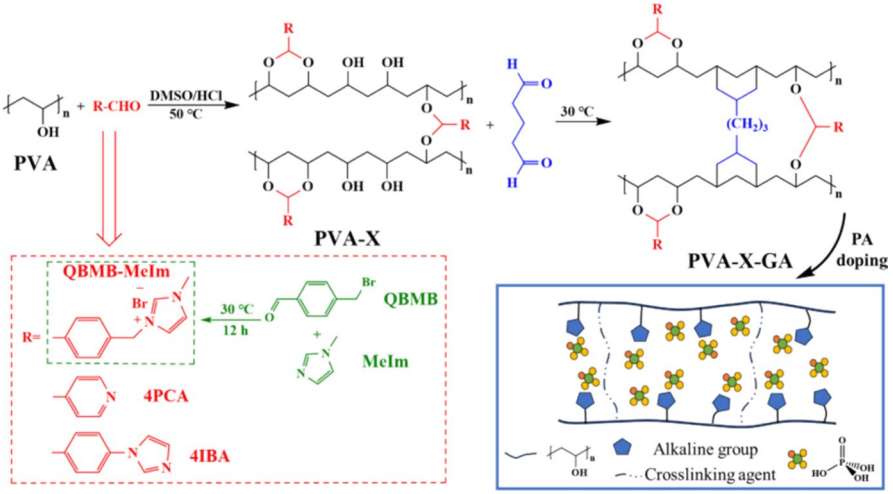

Fig. 1 Schematic preparation of PVA grafted and cross-linking membrane

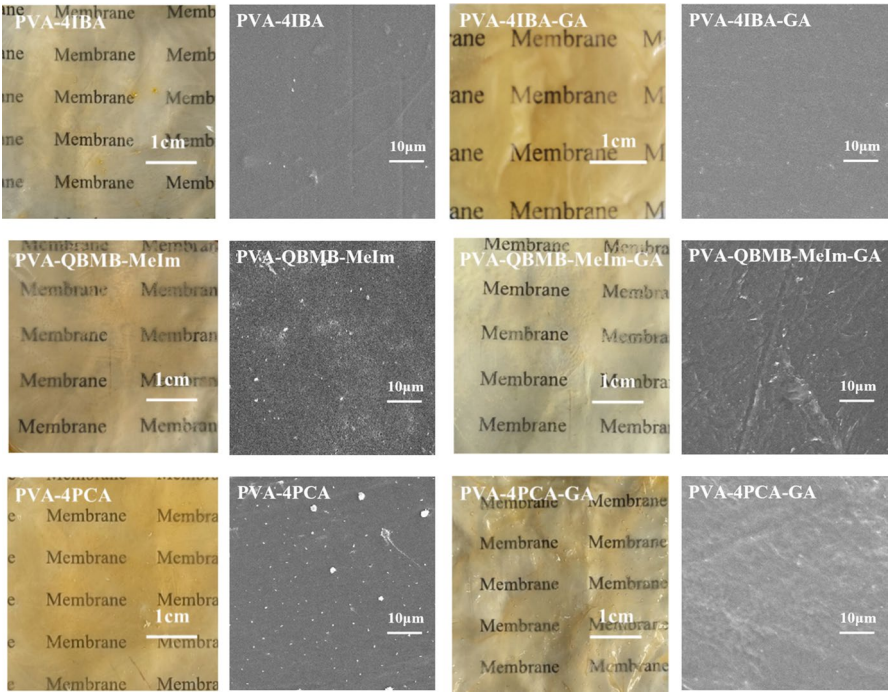

Fig. 2 Photographic and SEM images of PVA grafting and crosslinking membranes

^{1}H NMR and FT-IR spectra

Initially, the molecular structures of PVA and its grafted polymers, namely PVA-4IBA and PVA-4PCA, were characterized using ^{1}H NMR spectroscopy. Due to poor solubility, the PVA grafted with QBMB was not characterized by ^{1}H NMR. As illustrated in Fig. 3A, the peaks appearing at around 1.4 ppm and 3.8 ppm corresponded to methylene and methine groups, consistent with previous reports [39]. The peaks in the range of 4.2–4.7 ppm were attributed to hydroxyl groups [22]. Compared to PVA, several new peaks appeared in the spectra of PVA-4IBA and PVA-4PCA. In the spectrum of the PVA-4IBA polymer, three additional hydrogen peaks were observed. The peaks at chemical shifts of 6.6 ppm and 7.1 ppm corresponded to hydrogen atoms on the side-chain benzene ring and imidazole groups, respectively. The peak corresponding to the methine proton connecting the benzene ring with two oxygen atoms was detected at 5.4 ppm. Similarly, in the spectrum of the PVA-4PCA polymer, three additional hydrogen peaks were observed. The peak at 5.7 ppm was assigned to the methylene proton, similar to that in PVA-4IBA. The peaks corresponding to the pyridine rings appeared at approximately 7.8 ppm and 8.7 ppm [40]. In summary, the ^{1}H NMR results confirmed the successful grafting of the polymers. Furthermore, based on peak area analysis, the grafting degrees of PVA-4IBA and PVA-4PCA were determined to be 15.1% and 15.0%, respectively. As the grafting degree could not be determined via ^{1}H NMR, it was calculated based on the measured IEC value of 0.70 mmol g^{-1}. Using the method described in [41], the grafting degree of PVA-QBMB-MeIm was estimated to be 18.7%, consistent with values for the other grafted membranes.

Furthermore, FT-IR spectroscopy was utilized to investigate chemical structures of grafted and crosslinked PVA membranes. As illustrated in Fig. 3B, the broad and strong peak at 3311 cm^{-1} was associated with the stretching vibration of O–H groups connected to the carbon chain [22]. In the spectrum of PVA-QBMB-MeIm-GA, the intensity of this O–H stretching peak was significantly reduced, indicating that PVA-QBMB-MeIm has successfully crosslinked with GA. The peaks observed at 1158–948 cm^{-1} corresponded to the characteristic stretching vibrations of C–O bonds

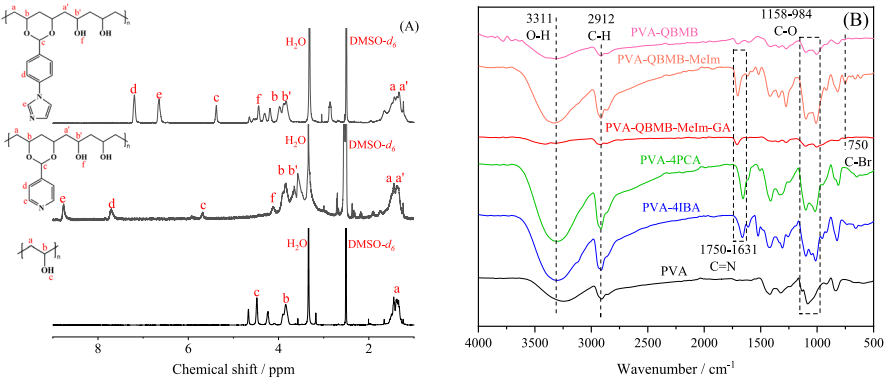

Fig. 3 **A** ^{1}H NMR spectra of PVA, PVA-4PCA and PVA-4IBA polymers and **B** FT-IR spectra of grafted and crosslinked PVA membranes

[20]. The characteristic peaks of the pyridine and imidazole rings were observed at 1750–1631 cm^{-1} associated with the stretching vibrations of C=N bonds [39, 42]. Additionally, absorption peaks at 2912 cm^{-1} were associated with the stretching vibrations of C–H bonds [22, 43]. Compared with PVA, the infrared spectrum of the PVA grafted with QBMB polymer showed a stretching vibration peak of C–Br at 750 cm^{-1} [20]. Therefore, FT-IR spectra further confirmed the successful grafting and crosslinking of PVA.

Thermal and chemical stabilities

Figure 4A presents the TGA curves of PVA and its grafted membranes. Pure PVA began to degrade at approximately 220 °C, while crosslinked membranes showed initial weight loss below this temperature, likely due to the decomposition of grafted side chains. However, all crosslinked membranes displayed minimal degradation (less than 5%) below 150 °C, indicating acceptable thermal stability for HT-PEM applications.

Figure 4B shows the chemical stability of various membranes in Fenton solution at 80 °C. It can be seen that all membranes retained 67–78% of their initial mass after 75 h. In addition, no disintegration was observed, indicating good oxidative stability.

Acid and water doping and swelling

The ADC% of HT-PEMs reflects the relationship between PA molecules and the membrane, affecting both the conductivity and structural integrity of the membrane [44, 45]. In order to eliminate the influence of membrane thickness on its performance, the thickness of all membranes was maintained at about 65 μm. Figure 5 illustrates the ADC% and dimensional swelling of different membranes immersed in 85 wt% PA. Because of the inclusion of pyridine and imidazole groups within the polymer chains, these membranes can interact with PA molecules through acid-base interactions and hydrogen bonding [38, 46]. As a result, the PVA-grafted and crosslinked membranes exhibit excellent PA absorption capacity. However, the ADC% of

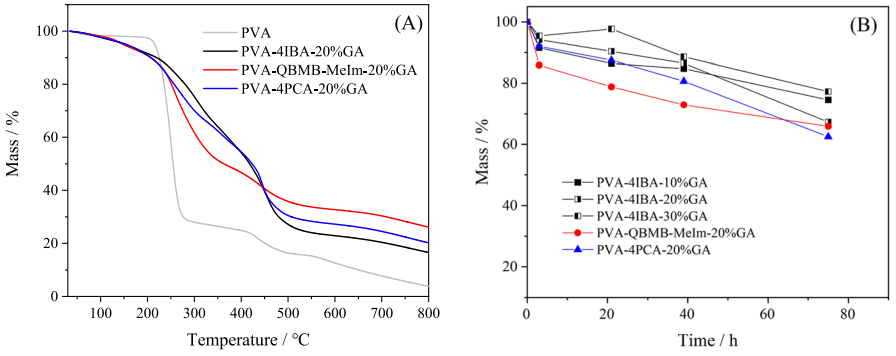

Fig. 4 **A** TGA curves of PVA and its cross-linked membranes at a heating rate of 10 °C min^{-1} under a nitrogen atmosphere; **B** The mass retention rate of various membranes in Fenton solution (3.0% H_2O_2 and 4.0 ppm Fe^{2+}) at 80 °C

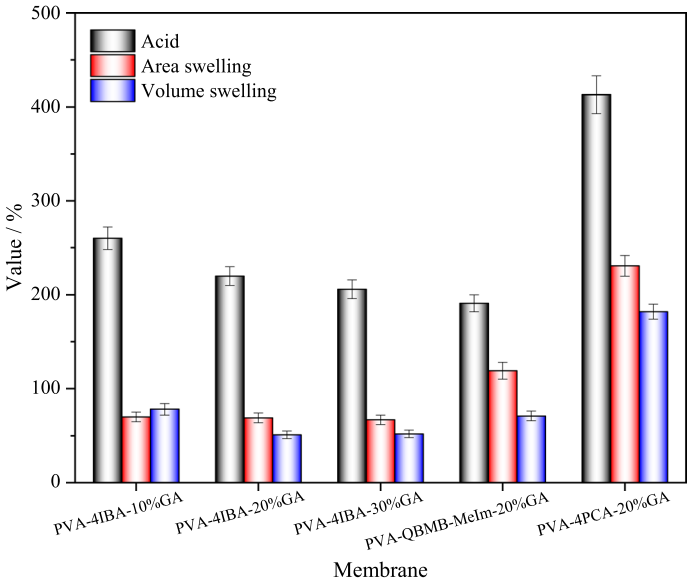

Fig. 5 ADC% and swellings of all crosslinked membranes after immersing 85 wt% PA solutions

the PVA crosslinked membranes decreased as the degrees of crosslinking increased. Of all the membranes studied, PVA-4PCA-20%GA membrane achieved the highest ADC% among all crosslinked membranes at 30 °C in 85 wt% PA solution. PVA-grafted membranes have excellent PA doping capacity, which may be attributed to their flexible backbone and the hydroxyl groups along the polymer backbone that can form hydrogen bonds [47]. As the degree of crosslinking increases, the quantity of hydroxyl groups along the polymer backbone decreases, and the flexibility of the polymer chain is reduced, leading to a decrease in the ADC% of the membranes.

Membranes with higher PA uptake typically exhibit noticeable swelling. Although elevated PA content improves proton conductivity, excessive swelling compromises dimensional stability, which can pose challenges under varying operational conditions of fuel cells, especially during long-term operation [48]. As shown in Fig. 5, PVA-4PCA-20%GA membrane immersed in 85 wt% PA at 30 °C showed area and volume swelling of 231% and 182%, respectively, and an ADC% of 413%. These values are significantly higher than those of the PVA-QBMB-MeIm-20%GA/191%PA membrane, which had area and volume swelling of 119% and 71%, respectively. This indicates that dimensional stability is significantly enhanced by the introduction of crosslinkers. The ADC% and swelling of PVA-4PCA-20%GA membranes were the highest when 20 wt% GA was used as the crosslinker. This suggests that when using the same crosslinking agent, different basic groups on the polymer side chains will also affect the ADC% and swelling of the membranes. The influence of different degrees of crosslinking and grafting groups on acid doping and swelling varies. Therefore, an appropriate degree of crosslinking and selection of grafting groups should be chosen to attain high ADC% while maintaining moderate dimensional stability.

Table 1 The water uptake, swelling performance in water and solubility in DMSO at 60 °C of various membranes

Membrane	WU (%)	WA (%)	WV (%)	MR (%)
PVA-4IBA-10%GA	40	7.8	8.9	69
PVA-4IBA-20%GA	25	3.6	4.6	87
PVA-4IBA-30%GA	18	1.4	5.6	86
PVA-QBMB-MeIm-20%GA	10	20.0	20.0	90
PVA-4PCA-20%GA	18	12.5	18.8	93

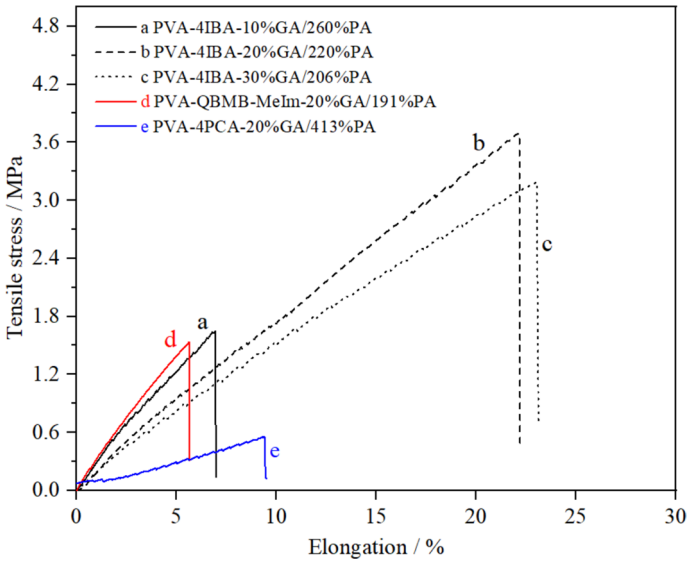

Fig. 6 Mechanical stress-strain curves of PA doped grafted and crosslinked PVA membranes at RT

Table 1 summarizes the water uptake and swelling behavior. As the degree of crosslinking increases, WU decreases, which aligns with the trend observed in ADC%. Notably, the PVA-QBMB-MeIm-20%GA membrane exhibited the lowest WU of 10%, while the PVA-4PCA-20%GA showed the highest swelling. In addition, the solubility of all cross-linked membranes in DMSO at 60 °C was also tested. All membranes showed high weight retention, indicating that the cross-linking network had been successfully formed in the PVA based membranes.

Mechanical properties

Outstanding mechanical strength is crucial for fabricating membrane electrode assemblies (MEAs) and ensuring the long-term performance of HT-PEMFCs [38]. Figure 6 shows the mechanical stress–strain curves for PA-doped PVA grafted and crosslinked membranes. Different degrees of crosslinking will have a significant impact on the mechanical properties of the membranes. With the increase of cross-linking degree, the structure of the membrane becomes denser, capable of accommodating fewer PA molecules, and the plasticizing effect of PA molecules and swelling effect are significantly reduced. Among all membranes, the PVA-4IBA-20%GA/220%PA membrane

with the ADC% of 220% exhibited the largest tensile strength of 3.7 MPa, which was similar to 3.2 MPa of the PVA-4IBA-30%GA/206%PA membrane. Because of the considerable plasticizing effect exerted by PA molecules, increased PA adsorption significantly reduces the tensile strength of the membranes [8]. However, PVA-4IBA-10%GA/260%PA membrane displayed a significantly reduced tensile stress at break of 1.6 MPa.

Proton conductivity

Figure 7 demonstrates the anhydrous conductivity of PA-doped PVA grafted and crosslinked membranes across a temperature range from 100 to 150 °C. Generally, increasing the temperature accelerates proton migration, thereby enhancing the conductivity of each membrane [49]. For example, the PVA-4IBA-20%GA membrane doped with 85 wt% PA at 30 °C exhibits a conductivity of 0.077 S cm^{-1} at 100 °C and 0.158 S cm^{-1} at 150 °C. As the degree of crosslinking increases, the conductivity of the membranes decreases to a certain extent generally. For instance, the PVA-4IBA-30%GA/206%PA membrane has a conductivity of 0.094 S cm^{-1} at 150 °C, whereas the PVA-4IBA-20%GA/220%PA membrane exhibits an increase in conductivity of 0.064 S cm^{-1} at 150 °C. On the contrary, the ADC% of the membrane PVA-4IBA-

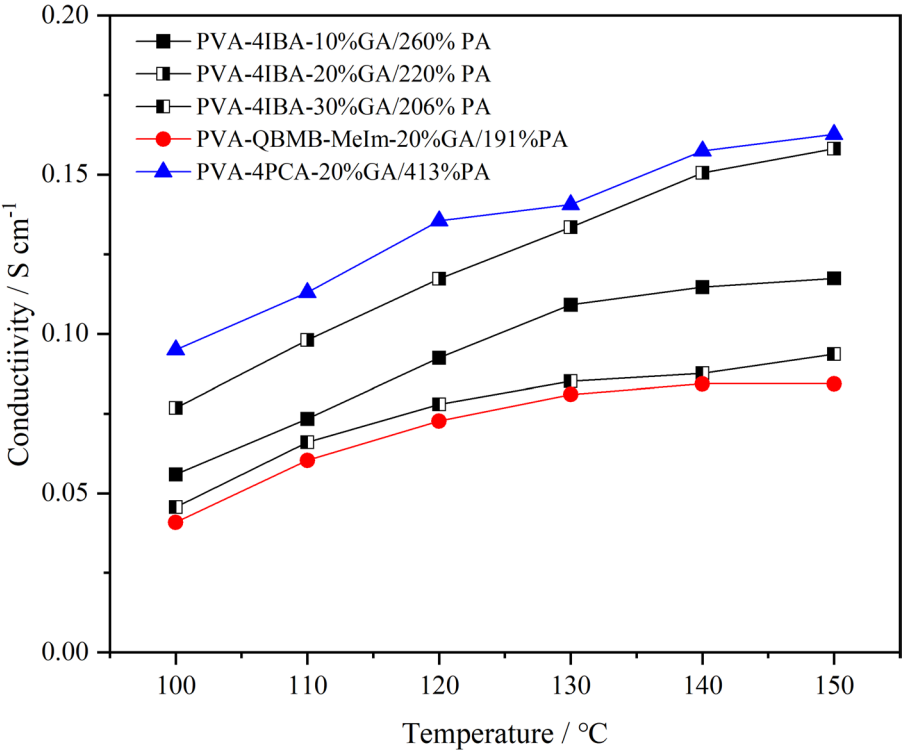

Fig. 7 Proton conductivities of PA doped grafted and crosslinked PVA membranes in relation to temperature

10%GA/260%PA is higher than that of the membrane PVA-4IBA-20%GA/220%PA, but its conductivity is smaller. It may be due to that part of PA is adsorbed in the gap of the network structure during doping, which makes the membrane swell and acid doped larger. However, in the process of high temperature drying, part of the PA is lost, making the ability of the PVA-4IBA-10%GA/260%PA membrane to transfer protons worse, so its conductivity is low [50]. When the degree of crosslinking is consistent, the PVA-4PCA-20%GA/413%PA membrane shows higher conductivity at a given temperature compared to the PVA-4IBA-20%GA/220%PA membrane, likely due to its higher ADC%. As noted earlier, an increased presence of PA molecules facilitates the formation of extensive dynamic hydrogen-bond networks and proton transport pathways, leading to increased conductivity [51]. In summary, the proton conductivity of PVA grafted and crosslinked membranes is influenced by the type of crosslinker and the functional groups grafted onto the polymer side chain. Considering the overall properties of the membranes discussed above, we believe that the PVA-4IBA-20%GA/220%PA membrane offers the best comprehensive performance and holds significant promise for application in HT-PEMFCs.

PA retention and comprehensive comparisons

The PVA-4IBA-20%GA membrane with the best comprehensive performance was selected for the PA retention test. As shown in Fig. 8, the PA retention rate of the PVA-4IBA-20%GA membrane decreased slightly and stabilized at ~73% after 17 h, indicating good acid-holding capacity. This can be attributed to the strong acid-base interactions between imidazole groups and phosphoric acid, as well as the dense network structure formed by glutaraldehyde crosslinking [52]. Meanwhile, the long-

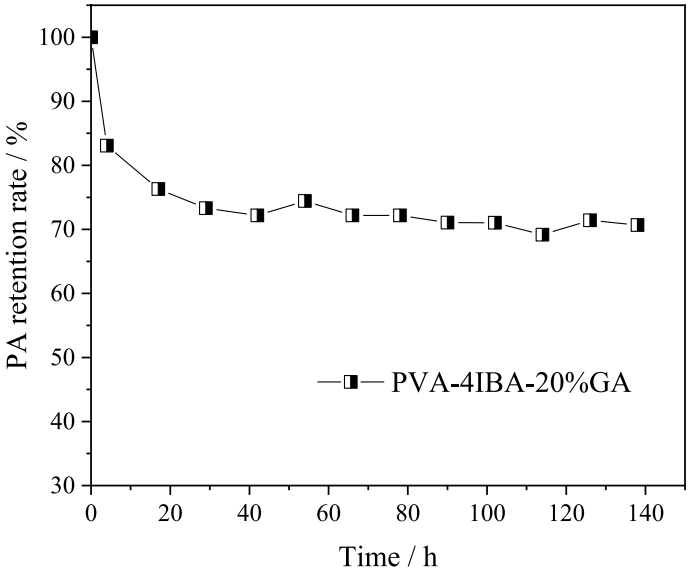

Fig. 8 The PA retention rate of PVA-4IBA-20%GA membrane under the conditions of 80 °C and 40% RH

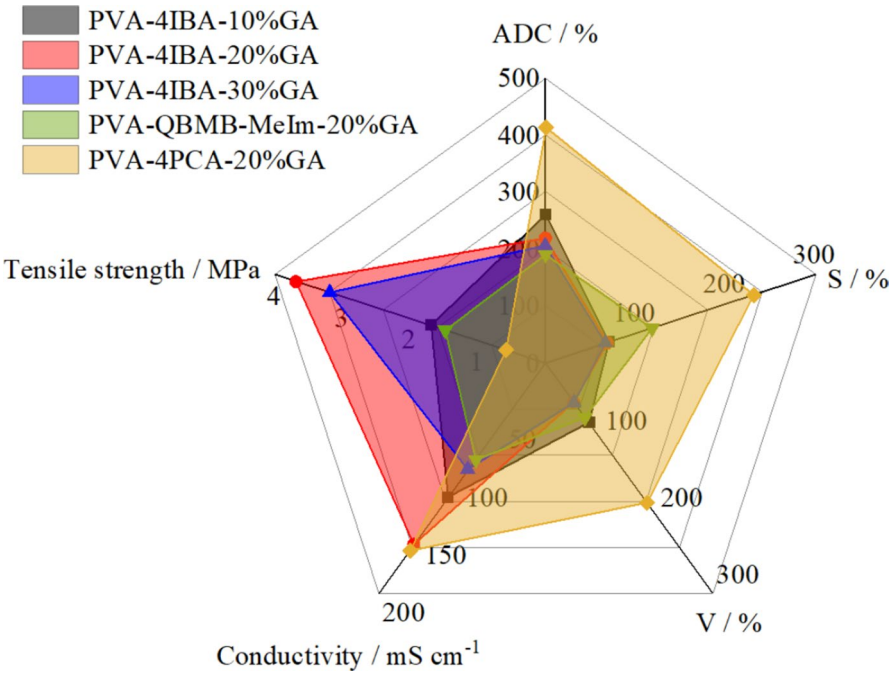

Fig. 9 Performance radar charts of various membranes

term conductivity stability of the PVA-4IBA-20%GA membrane was evaluated. As shown in Fig. S3, the conductivity initially decreased significantly within the first hour, likely due to membrane deformation at high temperature. Thereafter, the conductivity stabilized at 0.09 S cm^{-1}, indicating that the membrane maintains reasonable proton conductivity under prolonged high-temperature conditions.

Figure 9 presents a comprehensive performance comparison of the membranes. It can be seen that the PVA-4IBA-20%GA membrane exhibits a well-balanced profile, with both high proton conductivity and mechanical strength, along with relatively low volume and area swelling ratios.

Conclusions

This study focused on synthesizing HT-PEMs using economical and film-forming PVA. Under mild conditions, three aldehyde compounds containing alkaline groups—4-(bromomethyl)benzaldehyde grafted with 1-methylimidazole, 4-pyridinecarboxaldehyde, and 4-(1H-imidazol-1-yl)benzenecarbaldehyde—were grafted onto the main chain of PVA. GA was employed as the crosslinking agent to enhance the tensile strength of the membranes. ^{1}H NMR and FT-IR spectroscopy demonstrated the successful synthesis of these PVA-based polymers, and SEM analysis showed the membranes had a compact yet porous structure. The polymer's chemical structure played a vital role in increasing PA doping capacity, with the introduction of alkaline groups

significantly boosting the acid doping ability. Among all the membranes, the PVA-4IBA-20%GA/220%PA membrane exhibited the best overall performance, with a tensile strength of 3.7 MPa and the conductivity of up to 0.158 S cm^{-1} at 150 °C, making it a promising candidate for HT-PEMFC applications. Additionally, this work offers valuable insights into the development of alkaline group-grafted PVA membranes for various energy storage and conversion systems.

Supplementary Information The online version contains supplementary material available at https://doi.org/10.1007/s00289-025-06184-6.

Acknowledgements We gratefully acknowledge the Fundamental Research Funds for the Central Universities of China (N2005026), the Natural Science Foundation of China (52403273), and the Student Training Project of Shenyang Medical College (20249072).

Author contributions Peiru Lv: Writing—original draft, Methodology, Investigation, Formal analysis, Conceptualization. Li Ning: Investigation, Data curation. Danni Wu: Software, Formal analysis. Qi Liao: Investigation. Jin Wang: Conceptualization, Writing—review & editing, Funding acquisition. Jingshuai Yang: Writing—review & editing, Writing—original draft, Supervision, Project administration, Funding acquisition, Conceptualization.

Data availability No datasets were generated or analysed during the current study.

Declarations

Competing interests The authors declare no competing interests.

References

1. Teixeira FC, Teixeira APS, Rangel CM (2022) New proton conductive membranes of indazole- and condensed pyrazolebisphosphonic acid-Nafion membranes for PEMFC. Renew Energy 196:1187–1196
2. Huang L, Xu H, Jing B, Li Q, Yi W, Sun S (2022) Progress of Pt-based catalysts in proton-exchange membrane fuel cells: a review. J Electrochem 28:2108061
3. Sazali N, Salleh WNW, Jamaludin AS, Razali MNM (2020) New perspectives on fuel cell technology: a brief review. Membranes 10:99
4. Jiao K, Xuan J, Du Q, Bao Z, Xie B, Wang B, Zhao Y, Fan L, Wang H, Hou Z, Huo S, Brandon NP, Yin Y, Guiver MD (2021) Designing the next generation of proton-exchange membrane fuel cells. Nature 595:361–369
5. Wu D, Peng C, Yin C, Tang H (2020) Review of system integration and control of proton exchange membrane fuel cells. Electrochem Energ Rev 3:466–505
6. Li Y, Li D, Ma Z, Zheng M, Lu Z, Song H, Shao W (2022) Performance analysis and optimization of a novel vehicular power system based on HT-PEMFC integrated methanol steam reforming and ORC. Energy 257:124729
7. Xu J, Xiao S, Xu X, Xu X (2022) Numerical study of carbon monoxide poisoning effect on high temperature PEMFCs based on an elementary reaction kinetics coupled electrochemical reaction model. Appl Energy 318:119214
8. Lv R, Jin S, Li L, Wang Q, Wang L, Wang J, Yang J (2024) The influence of comonomer structure on properties of poly (aromatic pyridine) copolymer membranes for HT-PEMFCs. J Membr Sci 701:122703
9. Zhu L, Li Y, Liu J, He J, Wang L, Lei J (2022) Recent developments in high-performance Nafion membranes for hydrogen fuel cells applications. Pet Sci 19:1371–1381

10. Chinese Society of Electrochemistry (2024) The top ten scientific questions in electrochemistry. J Electrochem 30:2024121
11. Yin C, Li J, Zhou Y, Zhang H, Fang P, He C (2018) Enhancement in proton conductivity and thermal stability in nafion membranes induced by incorporation of sulfonated carbon nanotubes. ACS Appl Mater Interfaces 10:14026–14035
12. Jamil A, Rafiq S, Iqbal T, Khan HAA, Khan HM, Azeem B, Hanbazazah AS (2022) Current status and future perspectives of proton exchange membranes for hydrogen fuel cells. Chemosphere 303:135204
13. Tellez-Cruz MM, Escorihuela J, Solorza-Feria O, Compañ V (2021) Proton exchange membrane fuel cells (PEMFCs): advances and challenges. Polymers 13:3064
14. Haider R, Wen Y, Ma Z, Wilkinson DP, Zhang L, Yuan X, Song S, Zhang J (2021) High temperature proton exchange membrane fuel cells: progress in advanced materials and key technologies. Chem Soc Rev 50:1138–1187
15. Mabrouk W, Ogier L, Vidal S, Sollogoub C, Matoussi F, Fauvarque JF (2014) Ion exchange membranes based upon crosslinked sulfonated polyethersulfone for electrochemical applications. J Membr Sci 452:263–270
16. Charradi K, Ahmed Z, Thmaini N, Aranda P, Al-Ghamdi YO, Ocon P, Keshk SMAS, Chtourou R (2021) Incorporating of layered double hydroxide/sepiolite to improve the performance of sulfonated poly(ether ether ketone) composite membranes for proton exchange membrane fuel cells. J Appl Polym Sci 138:e50364
17. Charradi K, Daoudi M, Chemek M, Ahmed z, Alzahrani AYA, Siai A, Chtourou R, Keshk SMAS (2022) Synthesis, characterization and optical properties of oxidized poly vinyl alcohol. ChemistrySelect 7:e202103273
18. Wong CY, Wong WY, Loh KS, Daud WRW, Lim KL, Khalid M, Walvekar R (2020) Development of poly (vinyl alcohol)-based polymers as proton exchange membranes and challenges in fuel cell application: a review. Polym Rev 60:171–202
19. Ding C, Qiao Z (2022) A review of the application of polyvinyl alcohol membranes for fuel cells. Ionics 28:1–13
20. Mu T, Liu R, Shi N, Wang G, Yang J (2023) Dual cross-linked poly(vinyl alcohol)-based anion exchange membranes with high ion selectivity for vanadium flow batteries. ACS Appl Polym Mater 5:7110–7119
21. Wang D, Wang Y, Wang J, Wang L (2019) Synthesized geminal imidazolium-type ionic liquids applying for PVA-FP/[DimL][OH] anion exchange membranes for fuel cells. Polymer 170:31–42
22. Lu W, Shao Z, Zhang G, Zhao Y, Yi B (2014) Crosslinked poly(vinylbenzyl chloride) with a macromolecular crosslinker for anion exchange membrane fuel cells. J Power Sour 248:905–914
23. Yuan C, Li P, Zeng L, Duan H, Wang J, Wei Z (2021) Poly(vinyl alcohol)-based hydrogel anion exchange membranes for alkaline fuel cell. Macromolecules 54:7900–7909
24. Ari GA, Simsek O (2020) Imidazolium functionalized poly(vinyl alcohol) membranes for direct methanol alkaline fuel cell applications. Polym Int 69:644–652
25. Ruan H, Yu L, Yao Y, Li J, Yan J, Liao J, Shen J (2022) Poly(vinyl alcohol)-based anion exchange membranes with improved antifouling potentials and reduced swelling ratios for electrodialysis application. Ind Eng Chem Res 61:11357–11367
26. Yang W, Yan J, Liu S, Zhou J, Liu J, Zhang Q, Yan Y (2021) Macromolecular crosslink of imidazole functionalized poly(vinyl alcohol) and brominated poly(phenylene oxide) for anion exchange membrane with enhanced alkaline stability and ionic conductivity. Int J Hydrog Energy 46:37007–37016
27. Rao AS, Rashmi KR, Manjunatha DV, Jayarama A, Shastrimath VVD, Pinto R (2021) Methanol crossover reduction and power enhancement of methanol fuel cells with polyvinyl alcohol coated Nafion membranes. Mater Today Proc 35:344–351
28. Charradi K, Chemek M, Slimi B, Ramadan AM, Alzahrani AYA, Chtourou R, Keshk SMAS (2023) Fabrication and characterization of polyvalent metals/oxidized polyvinyl alcohol hybrid films with improved proton conductivity and optical performances. J Polym Environ 31:3167–3181
29. Pivovar BS, Wang Y, Cussler EL (1999) Pervaporation membranes in direct methanol fuel cells. J Membr Sci 154:155–162
30. Ye YS, Rick J, Hwang BJ (2012) Water soluble polymers as proton exchange membranes for fuel cells. Polymers 4:913–963

31. Kacem IB, Mabrouk W, Charradi K, Bellakhal N, Marzouki R, Raouafi N, Keshk SMAS (2024) Enhancing the performance of proton exchange membranes: incorporating layered double hydroxides into low sulfonated polyether sulfone octyl sulfonamide composite membranes. Mater Chem Phys 316:129119
32. Jin Y, Wang T, Che X, Dong J, Liu R, Yang J (2022) New high-performance bulky N-heterocyclic group functionalized poly (terphenyl piperidinium) membranes for HT-PEMFC applications. J Membr Sci 641:119884
33. Yang J, Jiang H, Wang J, Xu Y, Pan C, Li Q, He R (2020) Dual cross-linked polymer electrolyte membranes based on poly (aryl ether ketone) and poly (styrene-vinylimidazole-divinylbenzene) for high temperature proton exchange membrane fuel cells. J Power Sour 480:228859
34. Mabrouk W, Charradi K, Lafi R, AlSalem HS, Maghraoui-Meherzi H, Keshk SMAS (2022) Augmentation in proton conductivity of sulfonated polyether sulfone octyl sulfonamide using sepiolite clay. J Mater Sci 57:15331–15339
35. Mabrouk W, Charradi K, Maghraoui-Meherzi H, Alhussein A, Keshk SMAS (2022) Proton conductivity amelioration of sulfonated poly ether sulfone octyl sulfonamide via the incorporation of montmorillonite. J Electron Mater 51:6369–6378
36. Peng Z, Wei T, Wang Q, Zhao Y, Yang J (2025) Fabrication and investigation of anion exchange membranes based on poly(terphenyl piperidonium) copolymers with dibenzothiophene or dibenzofuran units for water electrolysis. J Power Sour 642:236918
37. Yang J, Wang Y, Yang G, Zhan S (2018) New anhydrous proton exchange membranes based on fluoropolymers blend imidazolium poly (aromatic ether ketone) s for high temperature polymer electrolyte fuel cells. Int J Hydrog Energy 43:8464–8473
38. Mu T, Wang L, Wang Q, Wu Y, Jannasch P, Yang J (2024) High-performance imidazole-containing polymers for applications in high temperature polymer electrolyte membrane fuel cells. J Energy Chem 98:512–523
39. Tang W, Yang Y, Liu X, Dong J, Li H, Yang J (2021) Long side-chain quaternary ammonium group functionalized polybenzimidazole based anion exchange membranes and their applications. Electrochim Acta 391:138919
40. Jin Y, Wang T, Che X, Dong J, Li Q, Yang J (2022) Poly (arylene pyridine) s: new alternative materials for high temperature polymer electrolyte fuel cells. J Power Sour 526:231131
41. Charradi K, Mabrouk W, Kacem IB, Bellakhal N, Al-Ghamdi YO, Marzouki R, Keshk SMAS (2024) Incorporation of multilayered double hydroxides/sepiolite augments proton conductivity performance in low sulfonated polyether sulfone octyl sulfonamide. Mater Renew Sustain Energy 13:97–107
42. Zhao B, Zhang Z, Zhang J, Wang L, Wang T, Dong J, Xu C, Yang J (2023) Long side-chain N-heterocyclic cation based ionic liquid grafted poly(terphenyl piperidinium) membranes for anion exchange membrane fuel cell applications. Polymer 286:126404
43. Yang J, Lv P, Tang W, Wang Q (2024) Sulfonate and ammonium-grafted poly (isatin triphenyl) membranes for the vanadium redox flow battery. ACS Appl Polym Mater 6:10727–10737
44. Che X, Wang L, Wang T, Dong J, Yang J (2023) The effect of grafted alkyl side chains on properties of poly(terphenyl piperidinium) based high temperature proton exchange membranes. Ind Chem Mater 1:516–525
45. Wang Q, Wang L, Zhang M, Peng Z, Lu Y, Lv P, Yang J (2024) Preparation of novel membranes with multiple hydrogen bonding sites and π-conjugated structure for high temperature proton exchange membrane fuel cells. Chem Commun 60:5318–5321
46. Jin Y, Liu R, Che X, Wang T, Yang J (2021) New high temperature polymer electrolyte membranes based on poly(ethylene imine) crosslinked poly(ether ketone cardo). J Electrochem Soc 168:054524
47. Wang L, Liu Z, Liu Y, Wang L (2019) Crosslinked polybenzimidazole containing branching structure with no sacrifice of effective N-H sites: towards high-performance high-temperature proton exchange membranes for fuel cells. J Membr Sci 583:110–117
48. Olsson JS, Pham TH, Jannasch P (2018) Poly(arylene piperidinium) hydroxide ion exchange membranes: synthesis, alkaline stability, and conductivity. Adv Funct Mater 28:1702758
49. Qu E, Hao X, Xiao M, Han D, Huang S, Huang Z, Wang S, Meng Y (2022) Proton exchange membranes for high temperature proton exchange membrane fuel cells: challenges and perspectives. J Power Sour 533:231386
50. Escorihuela J, García-Bernabé A, Compañ V (2020) A deep insight into different acidic additives as doping agents for enhancing proton conductivity on polybenzimidazole membranes. Polymers 12:1374

51. Wu A, Liu J, Huang J, Min Y, Wang Y, Wang S, Wang L (2022) Constructing high-density hydrogen bonding networks via introducing the bipyridine group for high-performance fuel cell proton exchange membranes. ACS Appl Energ Mater 5:11815–11824
52. Bin J, Peng J, Liu W, Huang H, Wang L, Luo J (2024) Achieving high cell performance based on block copolymer PBI membrane with strong acid absorbing Py-PBI segments. J Membr Sci 709:123111